An optical study of vacuum evaporated $Se_{85-x}Te_{15}Bi_x$ chalcogenide thin films

Ambika [*], P.B. Barman

Department of Physics, Jaypee University of Information Technology, Waknaghat, Solan, H.P. (173215), India

A B S T R A C T

Thin films of $Se_{85-x}Te_{15}Bi_x$ ($x = 0, 1, 2, 3, 4, 5$) glassy alloys prepared by melt quenching technique, are deposited on glass substrate using thermal evaporation technique under vacuum. The analysis of transmission spectra, measured at normal incidence, in the spectral range 400–1500 nm helphelps us in the optical characterization of thin films under study. Well -known Swanepoel's method is employed to determine the refractive index (n) and film thickness (d). The increase in n with increasing Bi content over the entire spectral range is related to the increased polarizability of the larger Bi atom (atomic radius 1.46 Å) compared with the Se atom (atomic radius 1.16 Å). Dispersion energy (E_d), average energy gap (E_0) and static refractive index (n_0) isare calculated using Wemple–DiDomenico model (WDD). The value of absorption coefficient (α) and hence extinction coefficient (k) hashave been determined from transmission spectra. Optical band gap (E_g) is estimated using Tauc's extrapolation and is found to decrease from 1.46 to 1.24 eV with the Bi addition. This behavior of optical band gap is interpreted in terms of electronegativity difference of the atoms involved and cohesive energy of the system.

© 2009 Elsevier B.V. All rights reserved.

1. Introduction

In recent years, the optical memory effects in chalcogenide semiconducting films have been investigated and utilized for various applications. The optical properties of chalcogenide vitreous semiconductors, i.e.., the excellent transmittance in the infrared region (in the wavelength regions 3–5 and 8–14 μm), continuous shift in the optical absorption edge, the variation in the refractive index under the influence of light and a very strong correlation between the former properties and the corresponding chemical composition, explains the significant interest in these amorphous materials for the manufacture of filters, anti -reflection coatings and in general, a wide variety of optical devices [1–3]. Due to their high refractive index (ranging between 2.0 and 3.5) and optical band gap lying in the sub-band gap region, chalcogenide glasses are used as core materials for optical fibers, which is are further used for transmission, especially when short length and flexibility is required [4–6]. Impurity effects in chalcogenide glasses have importance in fabrication of glassy semiconductors. These impurity atoms are supposed to satisfy all the valence requirements when they enter the glassy network and, therefore, not supposed to play the role of acceptors or donors. The effect of impurity atoms in chalcogenide glasses depends upon the composition of the glasses, the chemical nature of impurity, and the value of impurity concentration. Several

authors [7–9] have reported the impurity effects in various chalcogenide glasses.

Amorphous selenium has been investigated extensively due to its wide commercial applications. Its applications like rectifiers, photocells, xerography and switching and memory, etc. made it very attractive in the field of devices. Pure Se has short lifetime and low sensitivity. This problem can be overcome by alloying it with certain elements, which in turn gives high sensitivity, high crystallization temperature and smaller aging effects [10,11]. The substitution of Te for Se partly breaks up the Se_8 ring structure and increases the chain fraction. More recently it has been pointed out that Se–Te has some advantages over amorphous Se as forfar as their use in xerography is concerned [12]. The addition of third element expands the glass forming area and also creates compositional and configurational disorder in the system. The addition of impurities like Bi has produced a remarkable change in the optical and electrical properties of chalcogenide glasses. The conductivity of chalcogenide glasses changes from p to n type due to Bi addition [13–16]. An increasing concentration of Bi in Se–Te glassy alloy is responsible for the band tailing and broadening of valence band, which is further known to reduce the width of optical band gap. The aim of the present investigation is to study the effect of Bi incorporation on the optical properties of Se–Te matrix. A straightforward method proposed by Swanepoel [17]], which is based on the use of extremes of the interference fringes of the transmittance spectrum, enables us to calculate the value of refractive index and film thickness. The thickness of film samples is kept sufficiently high in order to obtain several interference fringes.

* Corresponding author. Tel.: +919817164795; fax: +911792245362.
E-mail address: ambikasharma2004@yahoo.co.in (Ambika).

2. Experimental details

Glasses of $Se_{85-x}Te_{15}Bi_x$, where $x = 0, 1, 2, 3, 4, 5$ were prepared by the melt quenching technique. The materials (5 N pure) were weighed according to their atomic percentages and sealed in evacuated (at $\sim 10^{-4}$ Pa) quartz ampoules. The sealed ampoules were kept inside a furnace, where the temperature was increased up to 1000 °C at a heating rate of 3–4 °C min^{-1}. The ampoules were frequently rocked for 15 h at the highest temperature to make the melt homogeneous. The quenching was done in ice-cold water. Glasses were obtained by breaking the ampoules.

Thin films of $Se_{85-x}Te_{15}Bi_x$ glasses were deposited on glass substrates, which are subjected to cleaning with soap solution, ultrasonically cleaning by trichloroethylene, acetone followed by methyl alcohol. Then, the substrate is washed by double -distilled water and dried in oven. Thin films of the alloys are prepared by thermal evaporation technique at $\sim 10^{-4}$ Pa base pressure in a vacuum coating system (HINDHIVAC 12A 4D model). Rate of evaporation was kept low (~ 10 Å s^{-1}) and thickness of film was controlled by thickness monitor (DTM 101). The bulk samples as well as their thin films have been characterized by the X-ray diffraction technique (Rigaku Geiger Flex 3KW Diffractometer) using Cu Kα source, and both were found to be amorphous in nature as no prominent peak was observed in their spectra. The transmission spectra of the thin films in the spectral range 400–1500 nm were obtained using a double beam ultraviolet–visible–near infrared spectrophotometer (Perkin Elmer, λ 750). The spectrophotometer was set with a slit width of 2 nm in the measured spectral range. All the measurements reported were taken at 300 K.

3. Results and discussion

3.1. Refractive index and film thickness

The transmission spectra of thin film samples under study are plotted in Fig. 1. The plot shows fringes due to interference at various wavelengths. A continuously oscillating maxima and minima at differe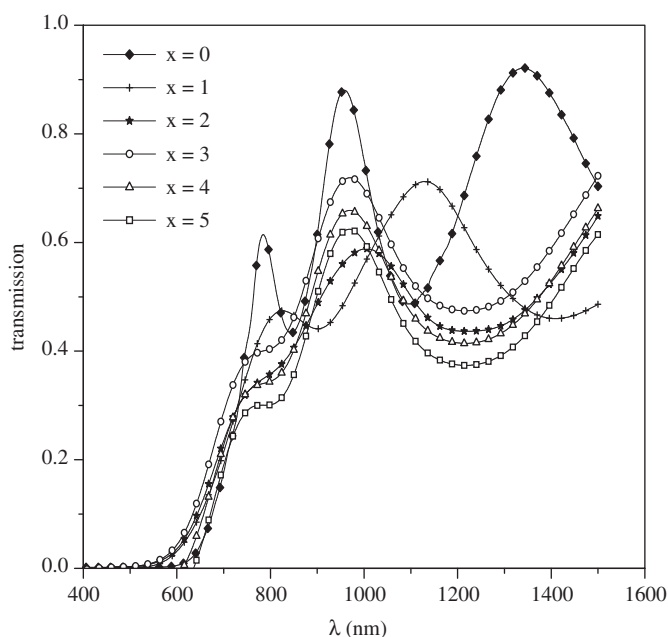nt wavelengths confirm the optical homogeneity of deposited thin films. According to SwanepoelSwanepoel's method, which is based on the idea of Manificier et al. [18] of creating upper and lower envelopes of transmittance spectrum, the refractive index, n of the film in the spectral region of weak absorption ($\alpha \approx 0$) is given by

$$n = [N + (N^2 - s^2)^{1/2}]^{1/2} \tag{1}$$

where

$$N = \frac{2s}{T_m} - \frac{(s^2 + 1)}{2} \tag{2}$$

In this equation, s (~ 15) is the refractive index of glass substrate and its values are obtained from transmission spectra of substrate T_s, using the relation [19]

$$s = \frac{1}{T_s} + \left(\frac{1}{T_s} - 1\right)^{1/2} \tag{3}$$

In the region of weak and medium absorption, where $\alpha \neq 0$, transmittance decreases mainly due to the effect of absorption coefficient, α and Eq. (2) modifies to

$$N = \frac{2s(T_M - T_m)}{T_M T_m} + \frac{s^2 + 1}{2} \tag{4}$$

where T_M and T_m are the transmission maximum and corresponding minimum at a certain wavelength λ.

If n_1 and $n_2 n_2$ are refractive indices of two adjacent maxima or two adjacent minima at wavelengths λ_1 and λ_2, respectively, then the thickness d_1 of the film is given by

$$d_1 = \frac{\lambda_1 \lambda_2}{2(\lambda_1 n_2 - \lambda_2 n_1)} \tag{5}$$

The average value of thickness, $\bar{d}_1$ for films under consideration is listed in Table 1. The accuracy of the above equation can also be increased by taking into consideration the basic interference equation

$$2nd_2 = m\lambda \tag{6}$$

where n is the order number, m is an integer for maxima and half integer for minima. The average value of thickness, $\bar{d}_2$ obtained from Eq. (6) is also incorporated in Table 1 and it has been observed that accuracy in determining the thickness of films is better than 2%.

The variation of n with wavelength for different composition of $Se_{85-x}Te_{15}Bi_x$, glassy alloys is shown in Fig. 2(a). It is clear from the figure that n decreasedecreases with an increase in the wavelength. This behavior is due to increase in transmittance and decrease of in absorption coefficient with wavelength. The decrease in refractive index with wavelength shows the normal dispersion behavior of the material. It is also evident from Fig. 2(a) that with the increase of in Bi content, n increases. This

Fig. 1. Plot of transmission versus wavelength (nm) for $Se_{85-x}Te_{15}Bi_x$ thin films.

Table 1
Values of refractive index (n), extinction coefficient (k) and dispersion energy (E_d), are given at 1100 nm and static refractive index (n_0), band tailing parameter (E_e), and average thickness (d) for $Se_{85-x}Te_{15}Bi_x$ ($x = 0, 1, 2, 3, 4, 5$) thin films.

x	n	k	$\bar{d}_1$ (nm)	$\bar{d}_2$ (nm)	E_d (eV)	n_0	E_e (eV)
0	2.88	0.0104	445	439	15.16	2.58	0.28
1	2.90	0.0349	477	468	15.78	2.67	0.40
2	2.94	0.0460	456	464	15.95	2.72	0.47
3	2.98	0.041	497	488	16.06	2.76	0.56
4	3.18	0.054	470	464	16.20	2.79	0.69
5	3.62	0.0637	498	492	16.70	2.83	0.89

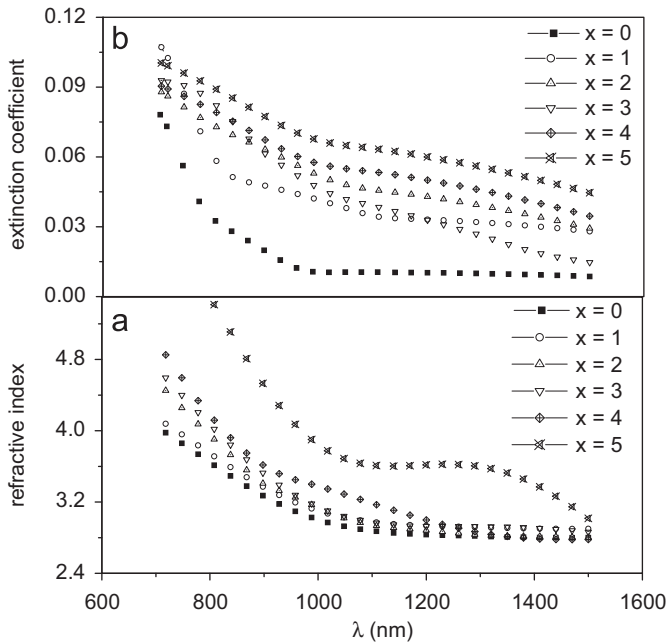**Fig. 2.** (a–b) Plot of refractive index (n) and extinction coefficient (k) versus wavelength (nm) for $Se_{85-x}Te_{15}Bi_x$ thin films.

increase is related to the increased polarizability of the larger Bi atomic radius 1.46 Å compared towith the Se atomic radius 1.16 Å [20]. The calculated value of n for thin films under study typically at 1100 nm is shown in Table 1.

3.2. Dispersion energy, oscillator strength and static refractive index from Wemple–DiDomenico model

The spectral dependence of the refractive index has been analyzed in terms of Wemple–DiDomenico (WDD) model [21], which is based on the single effective oscillator approach having the expression

$$n^2 - 1 = \frac{E_d E_0}{E_0^2 - (hv)^2} \qquad (7)$$

where hv is the photon energy, E_0 is the single oscillator energy (also called average energy gap) and E_d is the dispersion energy, which is a measure of average strength of the interband optical transitions. The oscillator parameters are determined by plotting refractive index factor $(n^2-1)^{-1}$ versus $(hv)^2$ and by fitting a straight line to the points as shown in Fig. 3. In Fig. 3, slope $= (E_0 E_d)^{-1}$ and the intercept on vertical axis $= (E_0/E_d)$. The value of E_d and E_0 are calculated using these two relations and are listed in Table 1 and Table 2, respectively. The parameter E_d is related to other physical parameters by simple empirical relation proposed by WDD model i.e. $E_d = \beta N_c Z_a N_e$, where β is a two - valued constant with either an ionic or covalent value ($\beta = 0.26 \pm 0.03$ eV for ionic materials and $\beta = 0.37 \pm 0.04$ eV for covalent materials), N_c is the effective coordination number of the cation nearest neighbor to anion, Z_a is the formal chemical valance of the anion and N_e is the effective number of valence electrons per anion. The increase in the observed value of E_d with Bi content is only due to the increase in the value of N_c and N_e. The single oscillator energy E_0, also known as WDD gap corresponds to the distance between centers of gravity of the valence and conduction band. It is therefore Therefore, it is related to the average bond strength or cohesive energy of the system. The cohesive energy (CE), defined as stabilization energy of an infinitely large cluster of the material per atom is determined by summing the bond
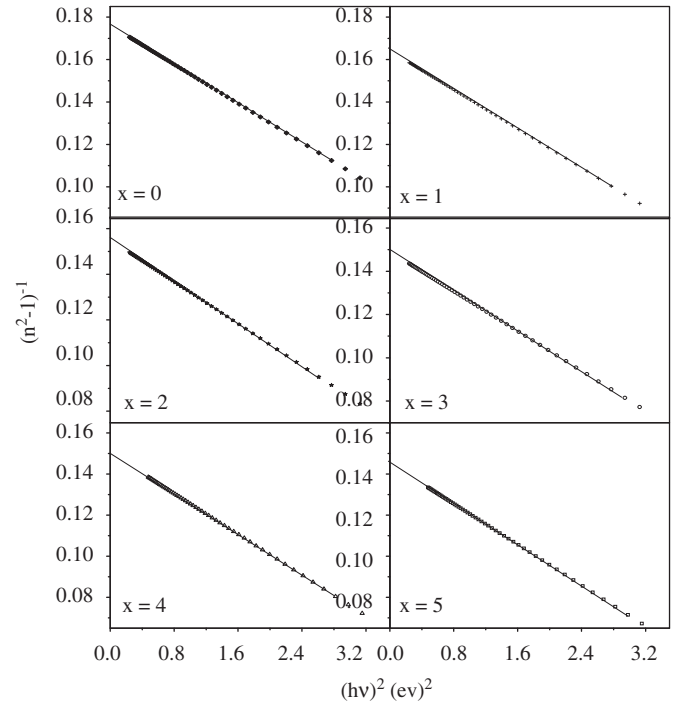

Fig. 3. Plot of $(n^2-1)^{-1}$ versus $(hv)^2$ for $Se_{85-x}Te_{15}Bi_x$ thin films.

Table 2
Excess Se–Se bonds, cohesive energy (CE), oscillator strength (E_0), and optical band gap (E_g) for $Se_{85-x}Te_{15}Bi_x$ ($x = 0, 1, 2, 3, 4, 5$) thin films.

x	Excess Se–Se bonds	CE (eV)	E_0 (eV)	E_g (eV)	ε_r	ε_i	σ (s^{-1})
0	140	2.76	2.68	1.46	9.63	0.0762	1.16×10^{13}
1	135	2.70	2.57	1.39	10.13	0.274	4.28×10^{13}
2	130	2.63	2.49	1.33	10.87	0.376	5.91×10^{13}
3	125	2.56	2.42	1.30	11.45	0.385	5.95×10^{13}
4	120	2.50	2.39	1.27	12.34	0.506	8.92×10^{13}
5	115	2.43	2.38	1.24	16.21	0.512	1.25×10^{13}

energies of the consequent bonds expected in the material. This behavior is equivalent to assuming a simplified model consisting of non -interacting electron pair bonds highly localized between adjacent pair of atoms. The cohesive energy (CE) of prepared bulk samples is evaluated using the relation [22]

$$CE = \sum (C_i D_i / 100) \qquad (8)$$

where C_i and D_i are the number of expected chemical bonds and energy of each bond, respectively. The bond energy of heteropolar bonds is calculated is by using PaulingPauling's method [23]. According to chemical bond approach (CBA) [24], atoms combine more favorably with atoms of different kind rather than with the same kind and bonds are formed in the sequence of decreasing bond energies until all the available valences are satisfied. Consequently, bonds between like atoms will only occur if there is an excess of certain type of atoms. In the above mentioned system, Bi is expected to combine preferably with Se because the bond energy of Bi–Se (170.4 kJ/mol) bond is higher than that of Bi–Te (125.6 kJ/mol). This results in decrease of in Se–Se (190.08 kJ/mol) bonds and is further responsible for lowering the average bond energy and hence, CE of the system. The excess Se–Se bonds and CE of the system is calculated and tabulated in Table 2.

The value of static refractive index n_0 has been calculated by extrapolating hv to zero in Fig. 3 and Eq. (7) reduces to

$$n_0 = (1 + E_d/E_0)^{1/2} \qquad (9)$$

The calculated values of static refractive index n_0, for films under investigation are given in Table 1.

3.3. Absorption coefficient, extinction coefficient and optical band gap

The absorption coefficient α, of $Se_{85-x}Te_{15}Bi_x$ thin films havehas been calculated by using the well -known relation

$$\alpha = \left(\frac{1}{d}\right) \ln \frac{1}{x} \qquad (10)$$

where x is the absorbance [8]. The extinction coefficient k, which is a measure of fraction of light lost due to scattering and absorption per unit distance of the participating medium is calculated using the relation $k = \alpha\lambda/4\pi$. Fig. 2(b) illustrates the dependence of k on the wavelength for different samples of thin films. The variation of $\ln(\alpha)$ with hv is shown in Fig. 4 and is found to increase with increase in photon energy. In amorphous semiconductors, the optical absorption edge spectra generally contain three distinct regions [25]:

(a) High absorption region ($\alpha = 10^4$ cm^{-1})), which involves the optical transition between valence band and conduction band and determines the optical band gap. The absorption coefficient in this region is given by

$$\alpha hv = B(hv - E_g)^p \qquad (11)$$

where E_g is defined as optical energy gap and B is a constant related to band tailing parameter. In the aboveabovementioned equation, $p = 1/2$ for a direct allowed transition, $p = 3/2$ for a direct forbidden transition, $p = 2$ for an indirect allowed transition and $p = 3$ for an indirect forbidden transition.
(b) Spectral region with $\alpha = 10^2$–10^4 cm^{-1} is called Urbach's exponential tail region in which absorption depends expo-

nentially on photon energy and is given by

$$\alpha hv = \alpha_0 \exp(hv/E_e) \qquad (12)$$

where α_0 is a constant and E_e is interpreted as band tail width of localized states, which generally represents the degree of disorder in amorphous semiconductor [26]. Fig. 4 shows a plot of $\ln(\alpha)$ as a function of hv and it helps in interpreting the value of E_e (see Table 1). In this region, most of the optical transitions take place between localized tail states and extended band states.
(c) The region ($\alpha \leq 10^2$ cm^{-1}) involves low energy absorption and originates from defects and impurities.

The optical energy gap (E_g), has been determined from absorption coefficient data as a function of photon energy (hv), using the Eq (11). After fitting all the values of p in the Tauc Tauc's relation, the value of p equals to 2 is found to hold good leading to indirect transitions [25].

The graph between $(\alpha hv)^{1/2}$ and hv for $Se_{85-x}Te_{15}Bi_x$ films is shown in the Fig. 5. The non -linear nature of the graph provides evidence that the transition in the forbidden gap is of indirect type. It is also evident from figure that optical band gap decreases with the addition of Bi content. This decrease in optical band gap may be correlated with the electronegativity difference of the elements involved. According to Kastner et al. [27], the valence band in chalcogenide glasses is constituted by lone pair p-orbital's contributed by the chalcogen atoms. These lone pair electrons will have a higher value of energies adjacent to electropositive atoms than those of electronegative atoms. Therefore, the addition of electropositive elements to the alloy may raise the energy of lone pair states, which is further responsible for the broadening of valence band inside the forbidden gap. The electronegativities of Se, Te and Bi are 2.4, 2.1 and 2.0, respectively. Since Bi is less electronegative than Se, the substitution of Bi for Se may raise the energy of some lone pair states, broadening the valence band. This leads to band tailing and hence shrinking of the band gap. It is also evident from Table 1 that band tailing parameter E_e increases with increasing Bi content, which may be due to the formation of structural defects like unsatisfied bonds. The concentration of
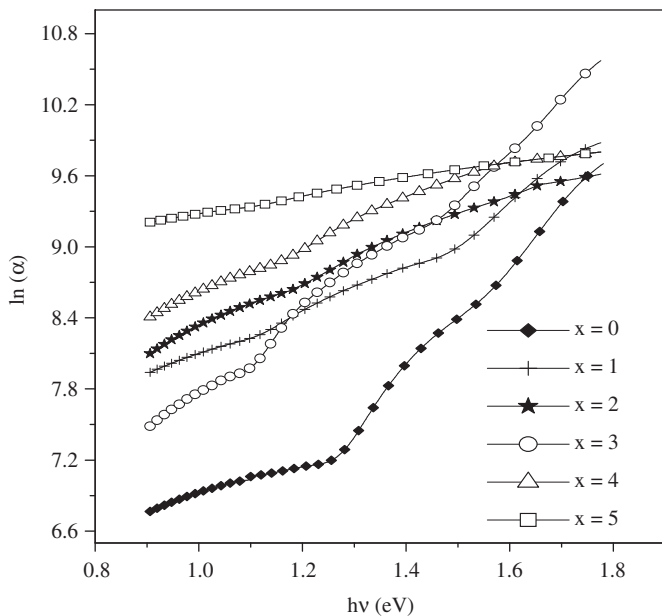

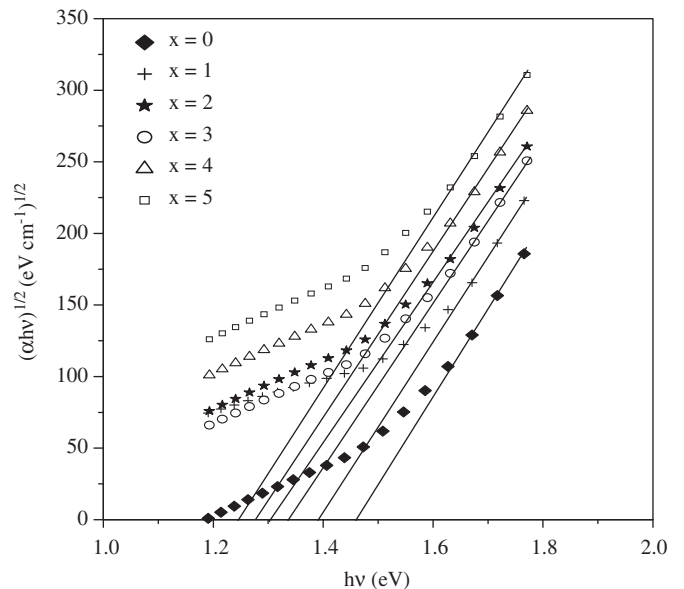**Fig. 4.** Plot of absorption ln (α) versus hv for $Se_{85-x}Te_{15}Bi_x$ thin films.

Fig. 5. Plot of $(\alpha hv)^{1/2}$ versus hv for $Se_{85-x}Te_{15}Bi_x$ thin films.

these defects also increases with Bi content. Therefore isolated centers of these defects can only introduce localized states at or near the band edges leading to an increase in the band tailing width. The values of band gap decreases from 1.46 to 1.24 eV as the Bi content is increased from 0 to 5 at% in the Se–Te glassy alloy. The optical band gap is a bond sensitive property [28]. Thus a decrease in optical band gap may also be explained on the basis of average bond energy of the system as explained earlier. Moreover the value of optical band gap E_g can be approximated using the oscillator energy value according to the relation $E_g = E_0/2$. The values are in good agreement with that derived from Tauc's extrapolation. The values of optical band gap for thin films under study are stated in Table 2. Similar trend of optical band gap with increasing Bi concentration have been observed by Suri et al. [29] while studying the optical properties of Se–Te–Bi glassy alloys. Moreover Ilyas et al. [30] also observed that the optical band gap decreases with increasing $Se_{98}Bi_2$ content in a-$(Se_{70}Te_{30})_{100-x}$ $(Se_{98}Bi_2)_x$ thin films.

The real (ε_r) and imaginary (ε_i) parts of the dielectric constants for a-$Se_{85-x}Te_{15}Bi_x$ thin films are calculated with the help of refractive index and extinction coefficient. Real part of dielectric constant is calculated using the relation $\varepsilon_r = n^2 - k^2$ while the imaginary part is calculated using, $\varepsilon_i = 2nk$. The variation of both ε_r and ε_i with $h\nu$ for thin films under consideration is shown in Fig. 6. For a-$Se_{85-x}Te_{15}Bi_x$ thin films, the variation of both ε_r and ε_i with $h\nu$ follows the same trend as that of refractive index and extinction coefficient. The optical conductivity is determined using the relation [21], $\sigma = \alpha nc/4\pi$ where 'c' is the velocity of light. Optical response is most conveniently studied in terms of optical conductivity and it has the dimensions of frequency, which are valid only in Gaussian system of units. The optical conductivity directly depends on the absorption coefficient and refractive index and is found to increase sharply for higher energy values due to large absorption coefficient as well as refractive index. The plots of optical conductivity versus wavelength for a-$Se_{85-x}Te_{15}Bi_x$ thin films are given in Fig. 7 and the variation of $\varepsilon_r, \varepsilon_i$ and σ (at $\lambda = 1100$ nm) with Bi at% is given in Table 2.
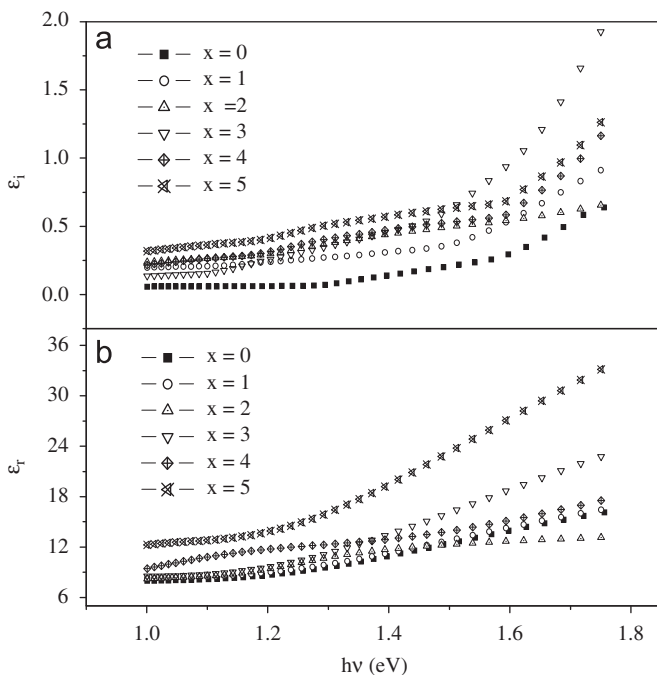

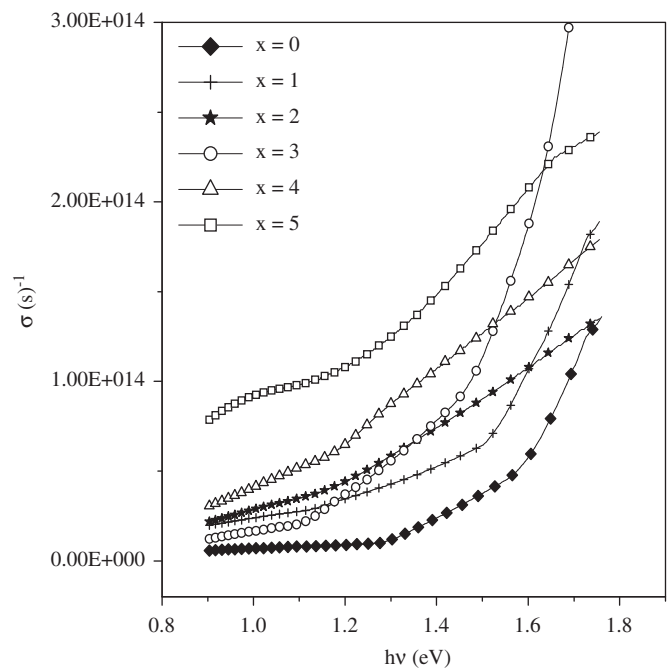**Fig. 7.** Plot of optical conductivity, σ versus $h\nu$ for $Se_{85-x}Te_{15}Bi_x$ thin films.

4. Conclusion

The transmission spectra of vacuum evaporated $Se_{85-x}Te_{15}Bi_x$ thin films taken at normal incidence have been analyzed in the spectral range 400–1500 nm and the various optical parameters are calculated. The refractive index and film thickness are calculated by using envelope method proposed by Swanepoel. The results indicate that n increases with the increasing Bi content, which is related to the increased polarizability of the larger Bi atomic radius 1.46 Å compared with the Se atomic radius 1.16 Å. The dispersion parameters E_d, E_0 and n_0 are discussed in terms of the WDD model. It has been observed that E_d and n_0 increases while E_0 decreases with increase in Bi content. The optical absorption in the given system seems to be of non -direct type and the optical band gap determined in the strong absorption region by Tauc's extrapolation is found to decrease from 1.46 to 1.24 eV by the addition of Bi content. The decrease in average bond energy and hence optical band gap is interpreted in terms of cohesive energy and electronegativity difference of the atoms involved. The dielectric constants and optical conductivity are determined for the system and they are found to follow the similar trend as that of refractive index.

Fig. 6. (a–b) Plot of dielectric constants, ε_r and ε_i versus $h\nu$ for $Se_{85-x}Te_{15}Bi_x$ thin films.

References

[1] A. Zakery, S.R. Elliott, J. Non- Cryst. Solids 330 (2003) 1.
[2] M.H.R. Lankhorst, Nature. Mater. 4 (2005) 347.
[3] M.A. Popesco, Non Crystalline Chalcogenides, Kluwer, Dordrecht, 2000.
[4] A. Elshafie, All A. Abdel, Physica B 269 (1999) 69–78.
[5] K. Abe, H. Takebe, K. Maronaga, J. Non- Cryst. Solids 212 (1997) 143.
[6] K. Wei, D.P. Machewirth, J. Wenzel, G.H. Sigel, J. Non- Cryst. Solids 182 (1995) 257.
[7] M.A. Majeed Khan, M. Zulfequar, M. Hussain, J. Phys. Chem. Solids 62 (2001) 1093.
[8] Ishu Sharma, S.K. Tripathi, P.B. Barman, J. of Phys D: Appl. Physics. 40 (2007) 4460–4465.
[9] E.R. Shaaban, M.A. Kaid, El Sayed Moustafa, A. Adel, J. Phys. D: Appl. Phys. 41 (2008) 125301.
[10] S.C.K. Mishra, T.P. Sharma, S.K. Sharma, R. Kumar, G. Jain, Indian J. Technol. 28 (1990) 205.

[11] S.A. Khan, M. Zulfequar, M. Hussain, Solid State Commun. 123 (2002) 463–468.
[12] H. Yang, W. Wang, S. Min, J. Non Cryst. Solids 80 (1986) 503.
[13] N. Tohge, Y. Yamamoto, T. Minami, M. Tanaka, J. Appl. Phys. Lett. 34 (1979) 640.
[14] N. Tohge, T. Minami, M. Tanaka, J. Non Cryst. Solids 59–60 (1983) 1015.
[15] P. Nagels, M. Rotti, W. Vikhrov, J. Phys. (Paris) 42 (1981) 907.
[16] P. Nagels, L. Tichey, A. Tiska, H. Ticha, J. Non Cryst. Solids 59–60 (1983) 999.
[17] E.R. Shaaban, Mater. Chem. Phys. 100 (2006) 411.
[18] J.C. Manifacier, J. Gasiot, J.P. Fillard, J. Phys. E: Sci. Instrum. 9 (1976) 1002.
[19] F.A. Jenkins, H.E. White, Fundamentals of Optics, McGraw-Hill, New York, 1957.
[20] E.R. Shaaban, M. Abdel-Rahman, El Sayed Yousef, M.T. Dessouky, Thin Solid Films 515 (2007) 3810.
[21] S.H. Wemple, M. DiDomenico, Phys. Rev. B 3 (1971) 1338.
[22] S.A. Fayek, M.R. Balboul, K.H. Marzouk, Thin Solid Films 515 (2007) 7281–7285.
[23] L. Pauling, Die Nature der Chemischen Bindung, VCH Weinheim, Berlin, 1976, pp. 80–89.
[24] J. Biecerano, S.R. Ovshinesky, J. Non Cryst. Solids 74 (1985) 75.
[25] J. Tauc, The Optical Properties of Solids, North-Holland, Amsterdam, 1970.
[26] M.M. Abdel-Aziz, E.G. El-Metwally, M. Fadel, H.H. Labib, M.A. Afifi, Thin solid films 386 (2001) 99.
[27] M. Kastner, D. Adler, H. Fritzsche, Phys. Rev. Lett. 37 (1976) 1504.
[28] A.K. Pattanaik, A. Srinivasan, J. Optoelectron Adv. Mater. 5 (2003) 1161.
[29] N. Suri, K.S. Bindra, M. Ahmad, J. Kumar, R. Thangaraj, Applied Physics. Phys. A, Materials and Processing. Process. 90 (2008) 149.
[30] M. Ilyas, M. Zulfequar, M. Husain, Optical Materials. Mater. 13 (2000) 397.